JOURNAL OF SOLID STATE CHEMISTRY 120, 223–230 (1995)

# Synthesis and Structure Approach of Barium-Oxomercurato(II)-Oxoruthenate(VI) $BaHgRuO_5$

Thomas Hansen, Armel Le Bail, and Yvon Laligant

*Laboratoire des Fluorures, CNRS URA 449, Université du Maine, Avenue O. Messiaen, 72017 Le Mans Cedex, France*

Received February 22, 1995; in revised form May 25, 1995; accepted June 8, 1995

**The new oxomercurate $BaHgRuO_5$ is synthesized under high oxygen pressure. Its structure is determined *ab initio* from conventional X-ray powder diffraction data by the direct methods. The cell is hexagonal (space group $P6_3/m$, $Z = 6$) with $a = 10.1760(1)$ Å and $c = 8.4121(1)$ Å. Electron microdiffraction confirms the Laue class. Refinements of 34 parameters by the Rietveld method using 541 reflections lead to $R_{Bragg} = 0.040$ and $R_p = 0.096$. The structure is built up from $RuO_5$ trigonal bipyramid groups sharing the two apical oxygen atoms exclusively with dumb-bell-like $HgO_2$ groups. Three of each of these groups form isolated $[OHgO(RuO_3)]_3$ rings between which are inserted the barium atoms either in tricapped trigonal prisms or icosahedron, both distorted. A relationship with the $Ba[RuO_3(OH)_2]$ structure is evidenced and discussed.** © 1995 Academic Press, Inc.

## INTRODUCTION

For a long time, only the oxomercurates $M_2HgO_2$ ($M$ = Li, Na, K, Cs) of alkaline metals were known (1). The existence of $CaHgO_2$ and $SrHgO_2$ was then reported (2), but the structures could not be determined. Many years later there was success in preparing monocrystals of $BaHgO_2$ (3), $SrHgO_2$ (4), and $Ho_2HgO_4$ (5) allowing their structure determination. At the same time, examinations of microcrystalline $CaHgO_2$, $SrHgO_2$ (6), and $Ln_2HgO_4$ ($Ln$ = La, Nd–Gd) (7) were communicated. Recently a new modification of $BaHgO_2$ was reported (8). The most recent publication of a ternary oxomercurate concerns $CdHgO_2$ (9) which could be obtained in form of monocrystals. Attempting the synthesis of mercury containing superconductors, first a nonsuperconducting substance $HgBa_2LnCu_2O_{6+\delta}$ (10) and then the superconducting phases $Ba_2HgCuO_{4+\delta}$ (11) and $Ba_2HgCa_3Cu_3O_{8+\delta}$ (12) were discovered.

Quaternary oxometalates of mercury with silver, palladium or platinum of the compositions $BaAg_2Hg_2O_4$ (13), $Ba_2Hg_3Pd_7O_{14}$ (14), and $BaHgPt_4O_{11}$ (15) were prepared under high pressure of oxygen. It is remarkable that under these conditions the higher oxidation states $Pd^{4+}$ and $Pt^{5+}$ could be stabilized. Further investigations of the Ba–Hg–$M$ oxide systems ($M$ = noble metal) led to the synthesis of a hitherto unknown phase containing Ba, Hg, Ru, and O, the structure of which is approached here by *ab initio* powder diffraction methodologies.

## EXPERIMENTAL PROCEDURES

Starting substances for the synthesis of $BaHgRuO_5$ were metallic ruthenium powder, mercury oxide and barium oxide, which were mixed in the molar relation 1:1:1, ground, and pressed into a pellet. The precursor was placed in an alumina crucible which was put into a quartz finger and heated for 8 days at 600°C in a closed special-steel (Ni–Co–Cr) container filled with condensed liquid oxygen. An oxygen pressure of more than 5000 bars could be maintained for 2 days by using a Bridgman sealing with a silver gasket which inhibited the decomposition of mercury oxide and led to the oxidation of ruthenium. Due to the weakening of the silver metal by heating, in the following 6 days the vessel lost gradually 500 bar each day down to 2000 bar when it was cooled down and opened. Probably because of the relatively low temperature used by constraints of the applied technique we did not obtain single crystals but only a black microcrystalline, air-stable powder. Due to technical problems it was furthermore not possible to synthesize a sufficient quantity for an examination by neutron diffraction. Application of other solid-state synthesis techniques, for example, experiments with sealed tubes of platinum or quartz at different temperatures between 500 and 900°C, for several hours up to a week, with different starting compounds and relations, did not lead to the desired compound.

The composition was characterized by energy dispersive X-ray analysis (EDX) performed first by a Leitz SR500 raster electron microscope with a LINK AN 10000 detector, then by a JEOL 2010 transmission electron microscope (TEM) equipped with a KEVEX energy dispersive X-ray spectrometer. An investigation of nearly 20 crystals revealed that their composition corresponds to $BaHgRuO_5$. Traces of nickel and strontium were also detected



0022-4596/95 $12.00

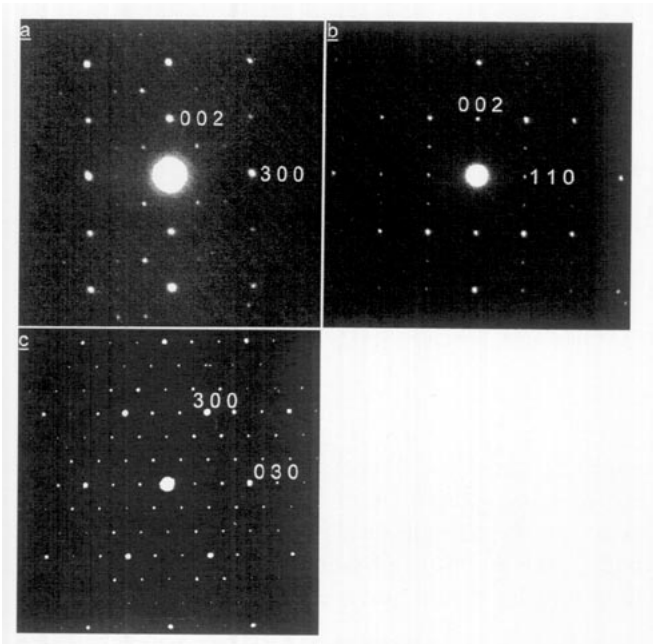


FIG. 1. Electron diffraction patterns of $BaHgRuO_5$ along (a) [1 $\bar{2}$ 0], (b) [1 $\bar{1}$ 0], and (c) [0 0 1].

at this stage certainly due respectively to contamination by the special-steel container and the starting barium oxide.

Thin specimens for electron microscopy were obtained by crushing and mounting the crystal fragments on a Cu grid covered with a carbon coated holey film. Electron diffraction was performed with the JEOL-2010 electron microscope operating at 200 kV and equipped with a side-entry ±30° double tilt specimen holder to explore reciprocal space.

The powder diffraction pattern was collected on a Siemens D501 diffractometer (Cu$K\alpha$, graphite diffracted beam monochromator, 38 kV, 28 mA, receiving slit 0.05°, angular range 9°–130° ($2\theta$), counting time 40 sec by steps of 0.02° ($2\theta$), room temperature, no sample rotation). Traces of $BaCO_3$ (Witherit, JCPDS file no. 44-1487) were detected, as well as by electron microscopy.

## STRUCTURE DETERMINATION

Chronologically, the cell was first obtained from the X-ray powder pattern by auto-indexing methods. This led to multiple possible space groups needing further TEM work. Electron diffraction, carried out with a number of crystals, which were rotated to scan the reciprocal space, showed the unit cell to be hexagonal with $a \approx 10.2$ Å and $c \approx 8.4$ Å. Electron diffraction pattern of the [1 $\bar{2}$ 0], [1 $\bar{1}$ 0], and [0 0 1] orientations are shown in Fig. 1 and allowed the deduction of the extinction symbol $P6_3$ - - compatible with the three space groups $P6_322$, $P6_3/m$, and $P6_3$ (Table 1).

The Laue class was then determined by electron diffraction by using the technique described by Morniroli and coworkers (16, 17). Images of the ⟨1 1 $\bar{2}$ 0⟩ ([1 $\bar{2}$ 1 0]) zone axes in Fig. 2 and ⟨1 $\bar{1}$ 0 0⟩ ([1 $\bar{1}$ 0 0]) zone axes in Fig. 3 allowed us to show the $P \cdot - -$ extinction symbol, the 0 0 0 l - l = $2n$ extinction condition leading to the $P6_3$ - - complete extinction symbol (Table 2). Images of the hexagonal plane, as shown in Fig. 4, reveal the absence of mirror planes which occur in the Laue class $6/mmm$. Therefore, only the less symmetric space groups $P6_3$ and $P6_3/m$ of Laue symmetry $6/m$ were considered (Table 2).

TABLE 1

| Reflection conditions | Extinction symbol | Laue Class | | |
|---|---|---|---|---|
| | | $6/m$ | | $6/mmm$ |
| | | Point group | | |
| 0001 | | 6 | $6/m$ | 622 |
| 1 | $P6_3$ -- | $P6_3$ (173) | $P6_3/m$ (176) | $P6_322$ (182) |

Concerning the X-ray powder pattern, the reflection positions were estimated by means of the program EVA (available in the Socabim PC software package DIFFRAC-AT supplied by Siemens, derivative method) after stripping $\alpha 2$. Auto-indexing was performed by using the program TREOR (18) applied to the first 20 detected lines. The most probable solution was hexagonal and character-

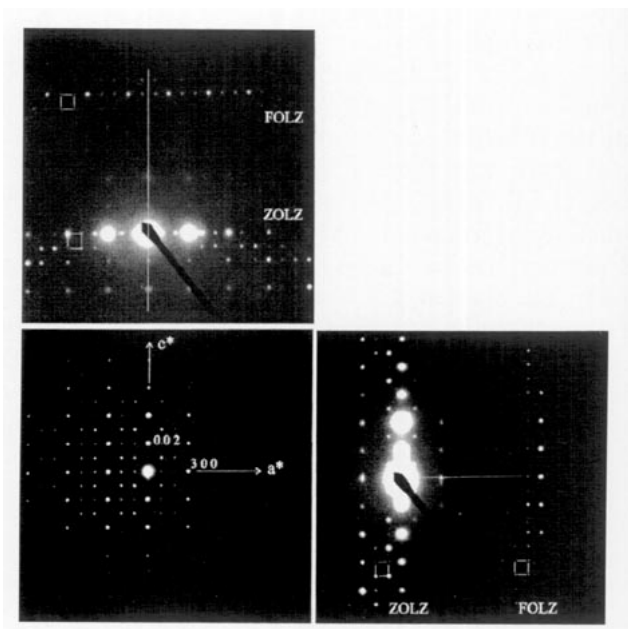


FIG. 2. [1 $\bar{2}$ 1 0] zone axes microdiffraction patterns of $BaHgRuO_5$ showing the whole pattern ($2mm$) "net" symmetry and the $P \cdot - -$ extinction symbol.

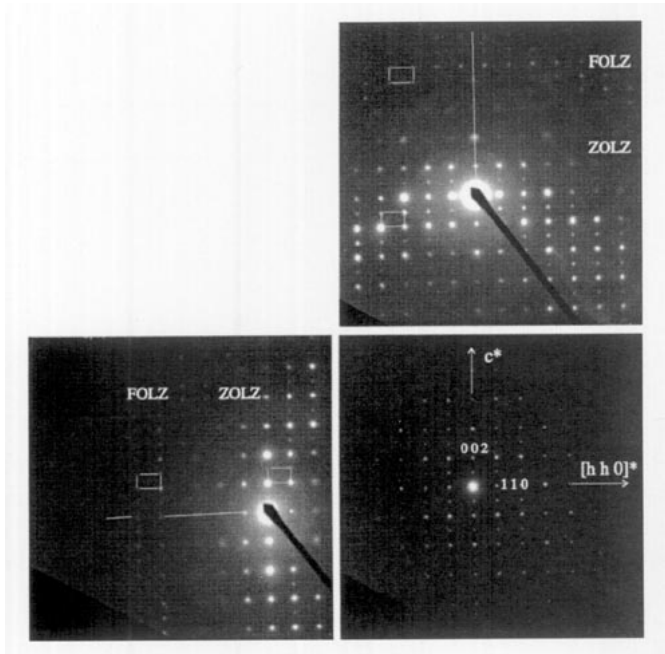


FIG. 3. [1 $\bar{1}$ 0 0] zone axes microdiffraction patterns of $BaHgRuO_5$ showing the whole pattern (2*mm*) "net" symmetry and the *P*··· extinction symbol.

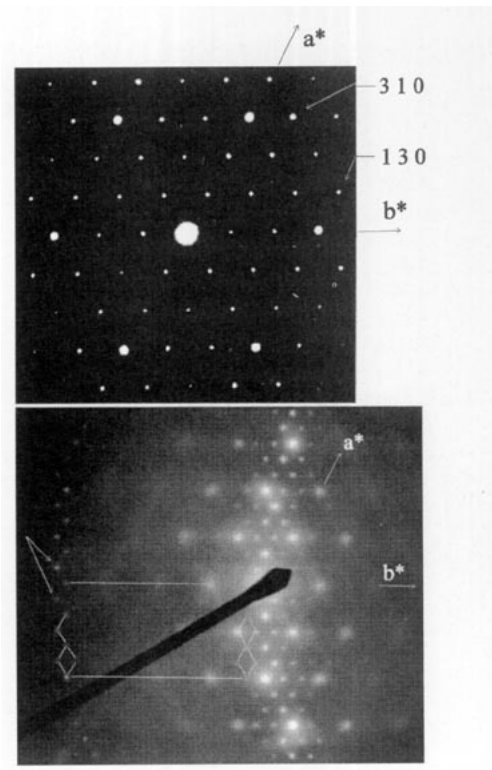


FIG. 4. (a) [0 0 0 1] "ZOLZ" pattern of $BaHgRuO_5$ showing the (6*mm*) "net" and (6) "ideal" symmetries. (b) [0 0 0 1] "FOLZ" microdiffraction pattern of the hexagonal $BaHgRuO_5$ phase obtained by tilting the incident beam around [0 0 0 1] showing the (6*mm*) "net" and (6) "ideal" symmetries.

ized by the conventional figures of merit $M_{20}$ = 41 and $F_{20}$ = 42 (0.016, 30) (19, 20).

The background correction was effectuated manually, as a consequence of the large bump on the pattern due to the amorphous contribution of the sample holder. In the 9°–130° (2$\theta$) angular range, a total of 541 "$|F_{obs}|$" amplitude structure factors were extracted by the Le Bail method (21) which consists in iterating the Rietveld (22) decomposition formula. Calculations were performed by the FULLPROF program (23). Equipartition was applied to the strictly overlapping reflections.

Then the direct methods from the SHELXS-86 program (24) permitted the location of the four heavy metal atom positions in the centrosymmetric space group $P6_3/m$ with the entire data set of 541 reflections. A total of 71 phases were observed for $|E|$ values greater than 1.2 and refined using 1545 unique triplets and 139 negative quartets (SHELXS-86 combined figure of merit 0.028). The solution produced an *E*-map with four peaks that were 2.5 to 6.4 times larger than the other ones. Atomic scattering factors and anomalous dispersion terms were taken from the "International Tables for X-ray Crystallography" (25). Alternating Rietveld refinements and Fourier syntheses with the program SHELXL-93 (26) unveiled progressively the positions of four oxygen atoms. Table 3 shows the X-ray powder diffraction data of $BaHgRuO_5$ with "observed" intensities from the final Rietveld refinement (FULLPROF). Table 4 gathers the conditions of data collection, the crystallographic characteristics, and the refined profile parameters together with the reliability factors for $BaHgRuO_5$. The barium carbonate impurity was treated by using the Le Bail method, including only those reflections having calculated intensities $I/I_{max} > 0.01$. Due to the very small quantity (about 50 mg) of material available, the sample could not intercept the whole incident beam at a low diffracting angle. A semiempirical correction was applied to take account of this problem. No improvement was obtained from refinements in the acentric $P6_3$ space group.

TABLE 2

| | Symmetries[a] | | | |
|---|---|---|---|---|
| | ⟨0 0 0 1⟩ Zone axis | | ⟨1 1 $\bar{2}$ 0⟩ Zone axis | ⟨1 $\bar{1}$ 0 0⟩ Zone axis |
| | N | I | N | N |
| ZOLZ | (6*mm*) | (6) | (2*mm*) | (2*mm*) |
| WP | 6*mm* | 6 | 2*mm* | 2*mm* |
| Extinction symbol | | | *P*··· | *P*··· |

[a] N denotes net and I denotes ideal.

TABLE 3
Powder Diffraction Data of $BaHgRuO_5$ ($CuK\alpha_1$; $\lambda$ = 1.54056 Å)

| $d_{obs}$ | $d_{calc}$ | $I_{calc}$ | "$I_{obs}$" | $h$ | $k$ | $l$ | $d_{obs}$ | $d_{calc}$ | $I_{calc}$ | "$I_{obs}$" | $h$ | $k$ | $l$ |
|---|---|---|---|---|---|---|---|---|---|---|---|---|---|
| 8.827 | 8.813 | <0.1 | <0.1 | 1 | 0 | 0 | | 2.0456 | <0.1 | <0.1 | 1 | 0 | 4 |
| 6.104 | 6.085 | 1.8 | 2.5 | 1 | 0 | 1 | | 2.0283 | 0.5 | 0.5 | 3 | 0 | 3 |
| 5.097 | 5.088 | 8.2 | 11.7 | 1 | 1 | 0 | 2.0205 | 2.0218 | 4.8 | 6.2 | 3 | 2 | 0 |
| | 4.406 | 3.7 | 3.2 | 2 | 0 | 0 | | 2.0218 | 1.4 | 1.7 | 2 | 3 | 0 |
| 4.359 | 4.354 | 65.6 | 79.5 | 1 | 1 | 1 | 1.9649 | 1.9658 | 0.2 | 0.2 | 3 | 2 | 1 |
| 4.210 | 4.210 | 145.5 | 171.2 | 0 | 0 | 2 | | 1.9656 | 7.9 | 7.1 | 2 | 3 | 1 |
| 3.9086 | 3.9033 | 3.9 | 4.8 | 2 | 0 | 1 | | 1.9516 | <0.1 | <0.1 | 4 | 0 | 2 |
| | 3.7959 | 0.2 | <0.1 | 1 | 0 | 2 | 1.9441 | 1.9435 | 1.2 | 1.1 | 1 | 1 | 4 |
| 3.3330 | 3.3309 | 7.0 | 6.9 | 1 | 2 | 0 | 1.9230 | 1.9231 | 1.4 | 1.4 | 4 | 1 | 0 |
| | 3.3309 | 10.2 | 10.1 | 2 | 1 | 0 | | 1.9231 | 0.3 | 0.3 | 1 | 4 | 0 |
| 3.2430 | 3.2418 | 986.0 | 1000. | 1 | 1 | 2 | | 1.8979 | 0.2 | 0.2 | 2 | 0 | 4 |
| 3.0969 | 3.0969 | 0.9 | 1.0 | 2 | 1 | 1 | 1.8840 | 1.8841 | 28.7 | 28.9 | 2 | 2 | 3 |
| | 3.0969 | 4.5 | 4.5 | 1 | 2 | 1 | 1.8743 | 1.8747 | 26.2 | 26.4 | 4 | 1 | 1 |
| | 3.0425 | <0.1 | <0.1 | 2 | 0 | 2 | | 1.8747 | 17.2 | 17.3 | 1 | 4 | 1 |
| 2.9378 | 2.9376 | 938.8 | 933.3 | 3 | 0 | 0 | 1.8424 | 1.8425 | 0.2 | 0.2 | 3 | 1 | 3 |
| | 2.7733 | <0.1 | <0.1 | 3 | 0 | 1 | | 1.8425 | 8.9 | 9.7 | 1 | 3 | 3 |
| 2.6724 | 2.6720 | 16.7 | 13.3 | 1 | 0 | 3 | 1.8212 | 1.8222 | 4.9 | 5.3 | 3 | 2 | 2 |
| 2.6128 | 2.6112 | 4.8 | 4.8 | 1 | 2 | 2 | | 1.8222 | 4.2 | 4.5 | 2 | 3 | 2 |
| | 2.6112 | 0.1 | 0.1 | 2 | 1 | 2 | | 1.7782 | 0.3 | 0.3 | 2 | 1 | 4 |
| | 2.5440 | 0.7 | 1.1 | 2 | 2 | 0 | | 1.7782 | 1.0 | 1.2 | 1 | 2 | 4 |
| 2.4557 | 2.4558 | 62.6 | 56.3 | 1 | 1 | 3 | | 1.7625 | 1.6 | 1.6 | 5 | 0 | 0 |
| | 2.4442 | 24.6 | 24.0 | 3 | 1 | 0 | 1.7489 | 1.7489 | 216.2 | 216.0 | 4 | 1 | 2 |
| | 2.4442 | 6.6 | 6.6 | 1 | 3 | 0 | | 1.7489 | 222.6 | 222.4 | 1 | 4 | 2 |
| 2.4360 | 2.4351 | 58.1 | 58.2 | 2 | 2 | 1 | | 1.7324 | 5.3 | 5.0 | 4 | 0 | 3 |
| 2.4083 | 2.4083 | 150.6 | 139.4 | 3 | 0 | 2 | | 1.7251 | <0.1 | <0.1 | 5 | 0 | 1 |
| | 2.3657 | 3.0 | 1.8 | 2 | 0 | 3 | 1.7099 | 1.7100 | 444.1 | 440.7 | 3 | 0 | 4 |
| 2.3470 | 2.3471 | 4.1 | 3.2 | 3 | 1 | 1 | 1.6958 | 1.6960 | 245.9 | 251.7 | 3 | 3 | 0 |
| | 2.3471 | 4.0 | 3.1 | 1 | 3 | 1 | 1.6653 | 1.6654 | 8.5 | 9.0 | 2 | 4 | 0 |
| | 2.2032 | 0.2 | 0.2 | 4 | 0 | 0 | | 1.6654 | 3.5 | 3.8 | 4 | 2 | 0 |
| 2.1768 | 2.1768 | 490.3 | 472.6 | 2 | 2 | 2 | | 1.6625 | 0.2 | 0.2 | 3 | 3 | 1 |
| 2.1442 | 2.1451 | 2.1 | 1.8 | 2 | 1 | 3 | | 1.6526 | 2.7 | 3.2 | 1 | 0 | 5 |
| | 2.1451 | 17.5 | 15.8 | 1 | 2 | 3 | | 1.6399 | 0.1 | 0.2 | 3 | 2 | 3 |
| 2.1323 | 2.1313 | 2.1 | 2.3 | 4 | 0 | 1 | | 1.6399 | <0.1 | <0.1 | 2 | 3 | 3 |
| | 2.1133 | 1.9 | 1.7 | 1 | 3 | 2 | 1.6337 | 1.6337 | 3.0 | 2.7 | 2 | 4 | 1 |
| | 2.1133 | 9.6 | 8.6 | 3 | 1 | 2 | | 1.6337 | 2.2 | 1.9 | 4 | 2 | 1 |

*Note.* The "observed" intensities are obtained by Rietveld refinement and the $d_{obs}$ by the EVA program.

## RESULTS AND DISCUSSION

The diffraction pattern plot is shown in Fig. 5. The atomic coordinates and thermal parameters are reported in Table 5. Selected interatomic distances and angles are listed in Table 6. As usual for X-ray powder structure calculations, one cannot expect a very high precision on the light atoms' positional parameters because of the presence of heavy scatterers. However, the mean metal–oxygen distances are roughly in agreement with the sum of ionic radii (27).

The crystal structure of $BaHgRuO_5$ viewed along the $c$ axis is shown in Fig. 6. The mercury atoms adopt a dumbbell-like twofold coordination (O(1)—Hg—O(3) almost aligned) which is also found in many other oxomercurates of alkaline and alkaline-earth metals (1–15). Further oxygen atoms appear with a distance of more than 2.64 Å to mercury.

Ruthenium is coordinated by five oxygen atoms forming a trigonal bipyramid as observed for other compounds of $Ru^{6+}$, for example, in $Ba[RuO_3(OH)_2]$ (28, 29), $K_2[RuO_3(OH)_2]$ (30, 31), and $CsK_5(RuO_5)(RuO_4)$ (32). For $Ru^{4+}$ and $Ru^{5+}$ only an octahedral coordination has been observed, with Ru—O distances between 1.9 and 2.0 Å. The fivefold coordination is the $Ru^{6+}$ characteristic, with three Ru—O distances of about 1.7 Å (the trigonal plane of a bipyramid) and two other distances of 2.0 Å (although a fourfold tetrahedral coordination has also been observed only for $Ru^{6+}$ (32), with Ru—O distances about 1.7 Å).

The barium atom Ba(2) is surrounded by nine oxygen atoms which form a twisted tricapped trigonal prism (Fig.

**TABLE 4**
**Conditions of Data Collection and Crystallographic Characteristics for $BaHgRuO_5$**

| | |
|---|---|
| Symmetry | Hexagonal |
| Space group | $P6_3/m$ (No. 176) |
| Cell parameters | $a = 10.1760(1)$ Å |
| | $c = 8.4121(1)$ Å |
| | $V = 754.38(1)$ Å$^3$ |
| | $Z = 6$ |
| Calculated density | 6.855 |
| Radiation | Cu$K\alpha$ |
| Data collection range | $9° \leq 2\theta \leq 130°$ |
| *Reflections measured* | *541* |
| Number of refined parameters | 34 |
| Halfwidth parameters | $U = 0.090(2)$, $V = -0.081(2)$, $W = 0.0416(6)$ |
| $\eta$ (pseudo-Voigt) | 0.32(1) |
| $\eta$ angular dependency | 0.0009(2) |
| Zeropoint | 0.0813(4)° ($2\theta$) |
| Asymmetry parameters | $P_1 = 0.223(3)$, $P_2 = 0.041(1)$ |
| Correction for low angle | sin $\theta$/sin $t$, $t = 35.5°$ |
| Reliability[a] factors with and | $R_P = 0.096$, $R_{WP} = 0.099$, $R_{Bragg} = 0.040$, $R_F = 0.040$ |
| without structure constraint | $R_P = 0.095$, $R_{WP} = 0.100$ |

[a] $R_P$ and $R_{WP}$ are the conventional Rietveld values, calculated after background subtraction.

**TABLE 5**
**Atomic Parameters and Isotropic Temperature Factors for $BaHgRuO_5$**

| Atom | Site | $x$ | $y$ | $z$ | $B_{iso}$ (Å$^2$) |
|---|---|---|---|---|---|
| Ba(1) | 2*a* | 0 | 0 | 0 | 0.27(2) |
| Ba(2) | 4*b* | $\frac{1}{3}$ | $\frac{2}{3}$ | 0.0165(2) | 0.27(2) |
| Hg | 6*c* | −0.0120(1) | 0.3216(2) | $\frac{1}{4}$ | 0.28(1) |
| Ru | 6*c* | 0.0124(2) | 0.6694(4) | $\frac{1}{4}$ | 0.04(3) |
| O(1) | 6*c* | 0.229(3) | 0.122(2) | $\frac{1}{4}$ | 2.0(2) |
| O(2) | 6*c* | 0.492(2) | 0.313(3) | $\frac{1}{4}$ | 2.0(2) |
| O(3) | 6*c* | 0.449(2) | 0.569(2) | $\frac{1}{4}$ | 2.0(2) |
| O(4) | 12*d* | 0.242(1) | 0.356(2) | 0.407(1) | 2.0(2) |

*Note.* $B_{iso}$ is the isotropic temperature factor. One $B_{iso}$ value was refined for all Ba atoms, the same for all O atoms.

7). Three O(2) oxygen atoms are building the smaller prism basal triangle (edges 2.9 Å) and three O(3) atoms build the other, wider triangle with edges of 3.3 Å. Barium is not at the center of this prism but is situated nearer to the latter triangle. Three O(4) oxygen atoms cap the rectangles of the trigonal prism. They are also nearer to the wider basal triangle than to the smaller. The barium atom Ba(1) centers a slightly deformed icosahedron built by six O(1) and six O(4) oxygen atoms (Fig. 7).

The $[HgO_2]^{2-}$ dumb-bells are connected by common oxygen atoms to two bipyramids $[RuO_5]^{4-}$. Each of these bipyramids shares the two opposite oxygen apical atoms with two dumb-bells, so that three bipyramids and three dumb-bells build up isolated rings (Fig. 8) with the $[HgO(RuO_3)O]_3$ formulation. The interconnection of these rings is ensured by the barium atoms. The coordinating oxygen atoms of Ba(2) belong to four rings, as demonstrated in Fig. 9. The described smaller triangle of O(2) belongs to one ring and is formed by the oxygen atoms,

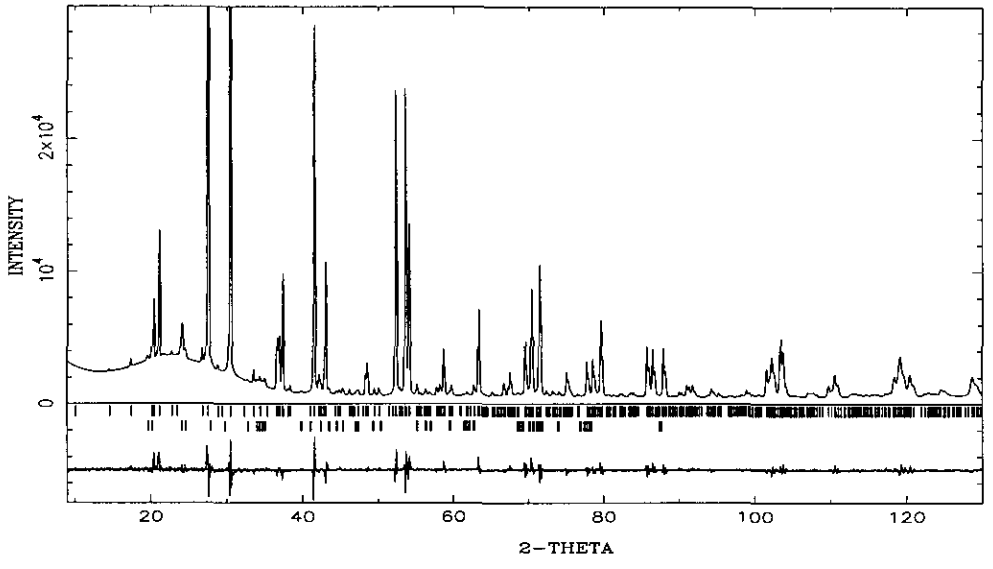


FIG. 5. Calculated powder pattern of $BaHgRuO_5$ and difference pattern (observed minus calculated). The vertical lines are the reflection positions of $BaHgRuO_5$ (above) and $BaCO_3$ (beneath). The two interrupted reflections culminate near $6 \times 10^4$ counts.

TABLE 6
**Main Interatomic Distances (Å) and Angles (°) in $BaHgRuO_5$**

| | $RuO_5$ trigonal bipyramid | | | | |
|---|---|---|---|---|---|
| Ru | O(4) | O(4) | O(2) | O(1) | O(3) |
| O(4) | **1.64(1)** | 2.64(2) | 3.09(3) | 2.67(3) | 2.51(2) |
| O(4) | 107(1) | **1.64(1)** | 3.09(3) | 2.67(3) | 2.51(2) |
| O(2) | 126.4(5) | 126.4(5) | **1.81(2)** | 2.40(3) | 2.85(4) |
| O(1) | 95.6(8) | 95.6(8) | 79(1) | **1.95(2)** | 3.94(3) |
| O(3) | 86.9(7) | 86.9(7) | 97(1) | 176(1) | **1.99(2)** |

| | $HgO_2$ dumb-bell | |
|---|---|---|
| Hg | O(1) | O(3) |
| O(1) | **1.89(3)** | 3.92(4) |
| O(3) | 175.9(8) | **2.03(2)** |

Hg–Ru intercationic distances
Hg Ru 3.383(3)
Ru 3.384(3)
Ru 3.422(5)

Next Hg–O distances
Hg O(2) 2.64(2)
O(4) 2.76(1) 2×
O(4) 3.04(1) 2×
O(2) 3.12(2)

Barium environment
Ba(1) O(1) 2.92(2) 6×
O(4) 3.30(2) 6×
Ba(2) O(3) 2.72(2) 3×
O(2) 2.80(1) 3×
O(4) 2.89(2) 3×

which lie in the plane of the ring (see Fig. 8) and are part of the trigonal base plane of the three trigonal bipyramids of $[RuO_5]^{4-}$. The other triangle of O(3) is built up by the three oxygen atoms which are part of $[HgO_2]^{2-}$ dumb-bells and $[RuO_5]^{4-}$ bipyramids of three different rings. Three oxygen atoms O(4) of these rings (which do not lie in the ring planes, but belong to the trigonal base planes of $[RuO_5]^{4-}$) cap the prism as described above. In this way, Ba(2) is connected to three $[RuO_5]^{4-}$ bipyramids by common edges as well as to three others and to three $[HgO_2]^{2-}$ dumb-bells by corner-sharing. The Ba(1) atoms share oxygen atoms with six different rings related by the $6_3$ screw axis.

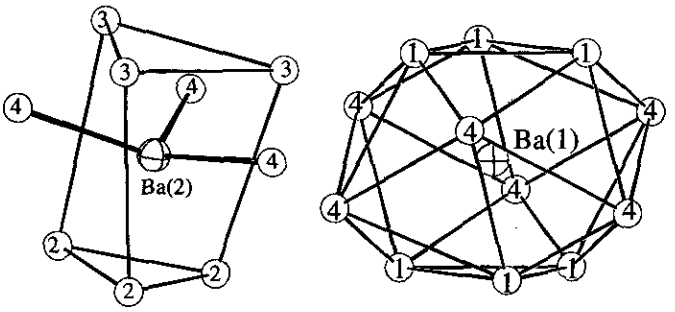


FIG. 7. $Ba(2)O_9$ (left) and $Ba(1)O_{12}$ (right) tricapped trigonal prism and icosahedron. The polyhedra share faces along the *c*-axis through O(3) and O(2) triangles for Ba(2)—Ba(2) and through O(1) triangles for Ba(1)—Ba(1) infinite piles.

Remarkable similarities between $BaHgRuO_5$ and $Ba[RuO_3(OH)_2]$ (28, 29) have been found. Although this oxide-hydroxide crystallizes in a rhombohedrical cell with a *c*-axis three times longer than that of the mercury compound, the relative positions of barium and ruthenium atoms are nearly the same in the two compounds. In $BaHgRuO_5$, mercury is a bridging cation in the rings of three ruthenium ions and their coordination sphere; in $Ba[RuO_3(OH)_2]$ this role is probably played by hydrogen bridges whose position could not be determined. However, it is highly probable that the two apical oxygen atoms, at 2 Å from the ruthenium, correspond to the $OH^-$ ions. In the hydroxide the rings' stacking order is different from that of $BaHgRuO_5$. The layers, which contain the $[(OH)RuO_3(OH)]_3$ rings, are piled as ... ABA'B'A"B" ... (Fig. 10), while in $BaHgRuO_5$ the order of the $[HgO(RuO_3)O]_3$ rings is rather simple with ... AB ... (so that ' and " indicate the *R* lattice translations).

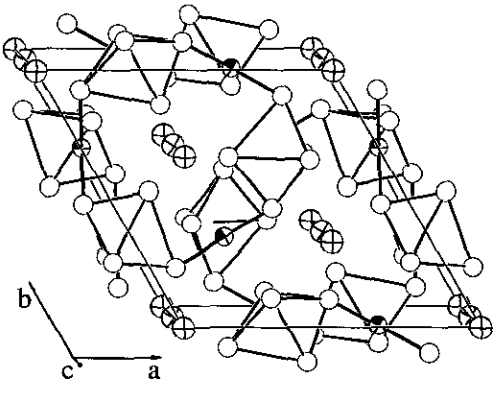


FIG. 6. Perspective view of the unit cell of $BaHgRuO_5$. Barium is drawn as large crossed circles, mercury as segmented spheres, and oxygen as empty circles. Ruthenium is represented as the $[RuO_5]^{4-}$ trigonal bipyramid and the dumb-bell-like coordination of mercury is shown by the bonds Hg–O.

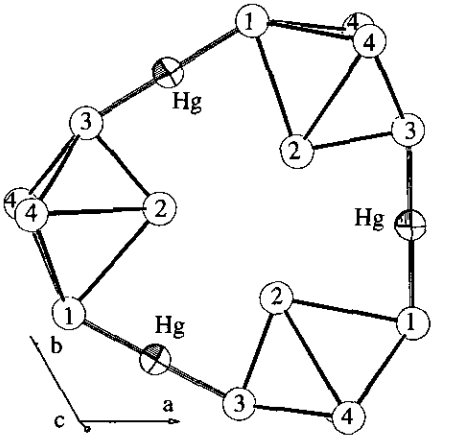


FIG. 8. Isolated ring $[HgO(RuO_3)O]_3$ of three trigonal bipyramids of oxygen around Ru atoms and three $HgO_2$ dumb-bells.

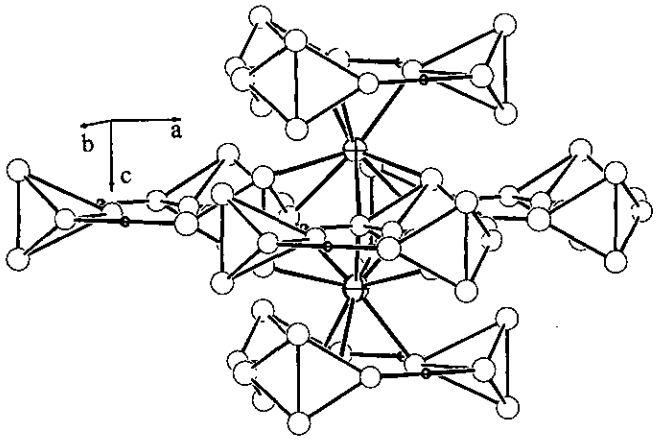


FIG. 9. Perspective view of the surrounding of the Ba(2) atom (large crossed spheres with bonds to oxygen) with $[HgO(RuO_3)O]_3$ rings (empty circles for oxygen, little crossed circles for mercury with bonds to oxygen, and bipyramids for the coordination spheres of ruthenium).

## SUMMARY AND CONCLUSIONS

It has been shown that synthesis with a high pressure of oxygen can lead to oxide compounds with high oxidation states that contain mercury.

A further demonstration of the powerful powder diffraction methodology for material characterization is made by the *ab initio* structure determination of $BaHgRuO_5$. Due to the small quantity available for this compound, neutron diffraction was not applicable. In spite of this drawback, we managed a structural approach to this hitherto unknown compound which shows a new structure type strongly related to $Ba[RuO_3(OH)_2]$.

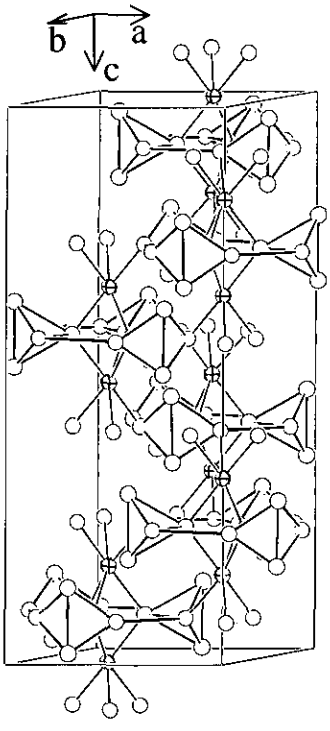


FIG. 10. Part of the unit cell of $Ba[RuO_3(OH)_2]$. The bipyramids around ruthenium are represented. Barium atoms, which are coordinated by the rings of three bipyramids, are drawn as crossed balls, with bonds to the six nearest oxygen atoms (empty circles). The positions of the supposed $OH^-$–oxygen are connected to show the similarity to mercury dumb-bells.

## ACKNOWLEDGMENTS

The crystal structure illustrations were created by a modified ORTEP program (33, 34) of the University of Kiel, Germany. One of the authors (Th. Hansen) thanks the European Union for a post-doctoral fellowship in the frame of the project "Human Capital and Mobility," Contract ERBCHBICT 941571.

## REFERENCES

1. R. Hoppe and H. J. Röhrborn, *Z. Anorg. Allg. Chem.* **329,** 110 (1964).
2. H. D. Wasel-Nielen, Dissertation, Universität Gießen, 1969.
3. M. Soll and Hk. Müller-Buschbaum, *J. Less-Common Met.* **162,** 169 (1990).
4. M. Soll and Hk. Müller-Buschbaum, *J. Less-Common Met.* **175,** 295 (1991).
5. M. Soll and Hk. Müller-Buschbaum, *J. Less-Common Met.* **170,** 321 (1991).
6. S. N. Putilin, M. G. Rozova, D. Kashporov, and E. V. Antipov, *Russ. J. Inorg. Chem.* **36,** 928 (1991).
7. S. N. Putilin, I. Bryntse, and M.G. Rozova, *J. Solid State Chem.* **93,** 236 (1991).
8. S. N. Putilin, S. M. Kazakov, and M. Marezio, *J. Solid State Chem.* **109,** 406 (1994).
9. Th. Hansen and Hk. Müller-Buschbaum, *Z. Anorg. Allg. Chem.* **620,** 1137 (1994).
10. S. N. Putilin, I. Bryntse, and E. V. Antipov, *Mater. Res. Bull.* **26,** 1299 (1991).
11. S. N. Putilin, E. V. Antipov, O. Chmaissem, and M. Marezio, *Nature* **362,** 226 (1993).
12. A. Schilling, N. Cantoni, J. D. Guo, and H. R. Ott, *Nature* **363,** 226 (1993).
13. M. Soll and Hk. Müller-Buschbaum, *Monatsh. Chem.* **122,** 915 (1991).
14. Th. Hansen and Hk. Müller-Buschbaum, *Z. Anorg. Allg. Chem.* **616,** 67 (1992).
15. Th. Hansen and Hk. Müller-Buschbaum, *Z. Anorg. Allg. Chem.* **620,** 1471 (1994).
16. J. P. Morniroli and J. W. Steeds, *Ultramicroscopy* **45,** 219 (1992).
17. A. Redjaïmia and J. P. Morniroli, *Ultramicroscopy* **53,** 305 (1994).
18. P.-E. Werner, L. Eriksson, and M. Westdhal, *J. Appl. Crystallogr.* **18,** 367 (1985).
19. P. M. De Wolff, *J. Appl. Crystallogr.* **1,** 108 (1968).
20. G. S. Smith and R. L. Snyder, *J. Appl. Crystallogr.* **12,** 60 (1979).
21. A. Le Bail, *NIST Spec. Publ.* **846,** 213 (1992).
22. H. M. Rieveld, *J. Appl. Crystallogr.* **2,** 65 (1969).
23. J. Rodriguez-Carvajal, "Program FULLPROF," Version 2.6.1, 1994.
24. G. M. Sheldrick, "SHELXS-86 Program User Guide," University of Göttingen, 1986.
25. "International Tables for X-ray Crystallography," (T. Hahn, Ed.), Vol. C. Kluwer Academic, Dordrecht, 1992.

26. G. M. Sheldrick, "Program SHELXL-93," University of Göttingen, 1993.
27. R. D. Shannon, *Acta Crystallogr. Sect. A* **32,** 751 (1976).
29. G. Nowogrocki, D. Thomas, and G. Tridot, *C. R. Acad. Sci. Paris C* **265,** 1459 (1967).
28. G. Nowogrocki, F. Abraham, J. Trehoux, and D. Thomas, *Acta Crystallogr.* **32,** 2413 (1976).
30. M. O. Elout, W. G. Haije, and W.J.A. Maaskant, *Inorg. Chem.* **27,** 610 (1988).
31. D. Fischer and R. Hoppe, *Z. Anorg. Allg. Chem.* **601,** 41 (1991).
32. D. Fischer and R. Hoppe, *Z. Anorg. Allg. Chem.* **617,** 37 (1992).
33. C. K. Johnson, Report ORNL-3794 Oak Ridge National Laboratory, Oak Ridge, T N, 1965.
34. K. B. Plötz, Dissertation, Universität Kiel, 1982.